analytical chemistry

Article

Cite This: Anal. Chem. 2018, 90, 3073−3078

pubs.acs.org/ac

Functional Dual-Color Indicator To Achieve in Situ Visualization of Intracellular Glycosylation

Yunlong Chen, Huipu Liu, Lin Ding, and Huangxian Ju*

State Key Laboratory of Analytical Chemistry for Life Science, School of Chemistry and Chemical Engineering, Nanjing University, Nanjing 210023, P. R. China

Supporting Information

ABSTRACT: A functional dual-color indicator is designed for in situ visualization of intracellular glycosylation. Using O-GlcNAcylation as model, the indicator is constructed on a poly-GlcNAc-coated gold nanoparticle (AuNP) by assembling dye labeled lectin (FSWGA) and then another dye-labeled GlcNAc (FGlcNAc) through the two opposite subunits of FSWGA. These dyes possess negligible overlapping emission and can be quenched by AuNP. In the presence of intracellular dissociated GlcNAc residue and O-GlcNAcylated proteins, the assembled FGlcNAc and the conjugate of FSWGA with FGlcNAc are released from AuNP through the dynamic competitive conjugation, which lights up the fluorescence of two dyes, respectively, and provides a simple technique for simultaneously monitoring the level of O-GlcNAcylated proteins and the total amount of GlcNAc groups in living cells. The practicality of the protocol for visually monitoring the biological pathway between intracellular O-GlcNAcylation and cell surface differentiation-related proteins demonstrates a convenient and powerful tool for research of glycosylation equilibrium and related biological processes.

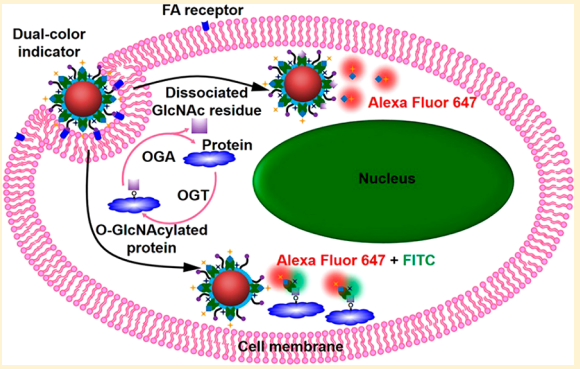

Glycosylation is one of the most important post-translational modification of proteins.[1] Many nuclear and cytoplasmic proteins are borne monosaccharide O-linked *N*-acetylglucosamine (O-GlcNAc) through serine or threonine, which is called as O-GlcNAcylation.[2] O-GlcNAcylation is essential for cell survival and plays important roles in many biological processes, such as transcription, translation, and cell division.[3] Abnormal O-GlcNAcylation of cellular proteins occurs in many kinds of cancers, indicating its association with malignancy.[4] Generally, the O-GlcNAcylation is dynamically regulated by two key enzymes: O-GlcNAc transferase (OGT)[5] and O-GlcNAcase (OGA),[6] which lead to the addition and removal of GlcNAc residue to/from proteins, respectively. The O-GlcNAcylated protein and dissociated GlcNAc residue take the main component of intracellular O-GlcNAcylation process, while other GlcNAc-related components, such as GlcNAc phosphates are very limited.[7] Thus, simultaneous monitoring of the levels of O-GlcNAcylated protein and dissociated GlcNAc residue within living cells is of great importance in revealing O-GlcNAcylation related biological processes and potential tumor progression.

The monitoring of O-GlcNAcylation level of specific protein in living cells has been achieved with in situ Förster resonance energy transfer (FRET) imaging[8] by labeling the GlcNAc with metabolic engineering fluorophore and the target protein with green fluorescent protein to give the FRET signal of target-related O-GlcNAcylation. However, this method cannot give the level of dissociated GlcNAc residue, and it is difficult to monitor the levels of all more than 1000 identified O-GlcNAcylated proteins.[9] Thus, the in situ visual protocol with an insight into intracellular OGT/OGA mediated O-GlcNAcylation is still an urgent demand.

To achieve a comprehensive survey of OGT/OGA mediated intracellular O-GlcNAcylation, this work designs a functional dual-color indicator for in situ simultaneous visual analysis of O-GlcNAcylated proteins and GlcNAc residue within living cells (Figure 1). This indicator is constructed on a poly-GlcNAc (PGlcNAc) coated gold nanoparticle (AuNP) (PGAu) by assembling fluorescent dye labeled succinylated wheat germ agglutinin (FSWGA) and then another fluorescent dye labeled GlcNAc (FGlcNAc) (Figure 1A). These fluorescent dyes possess negligible overlapping emission and are quenched by the AuNP. Polyethylene glycol terminated with sulfhydryl and folic acid (HS-PEG-FA) is also doped on its surface to improve its stability and endocytosis efficiency. FSWGA possesses a dimeric-subunit structure to respectively connect PGlcNAc and FGlcNAc.[10−13] Different from the native wheat germ agglutinin,[14] FSWGA contains partially obstructed binding sites on each subunit by succinylation to keep its specificity to GlcNAc.[15] The competitive binding of free GlcNAc residue to the outside subunit leads to the release of FGlcNAc and thus

Received: September 1, 2017
Accepted: February 8, 2018
Published: February 8, 2018

DOI: 10.1021/acs.analchem.7b03587
Anal. Chem. 2018, 90, 3073−3078

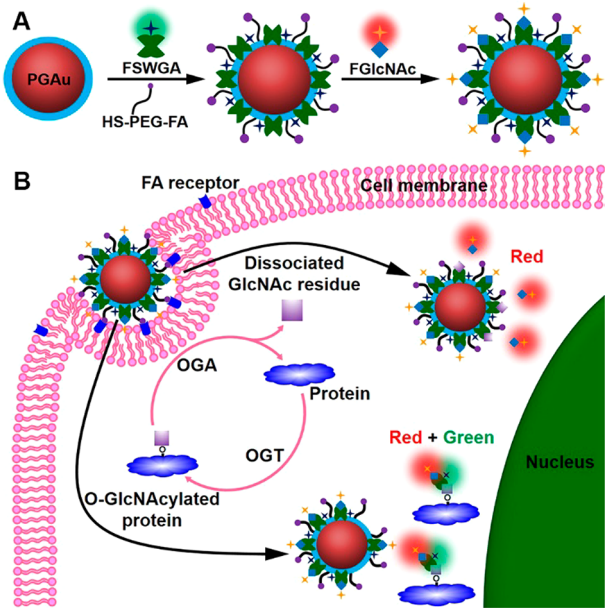

Figure 1. Schematic illustration of (A) preparation of functional dual-color indicator and (B) in situ visualization of intracellular O-GlcNAcylation.

lights up the red fluorescence of Alexa Fluor 647 on FGlcNAc. Meanwhile, O-GlcNAcylated proteins can competitively bind the inside subunit of FSWGA, which releases the conjugate of FSWGA with FGlcNAc to light up both the green fluorescence of fluorescein isothiocyanate (FITC) on FSWGA and red fluorescence of FGlcNAc (Figure 1B). As a proof of concept, breast cancer MCF-7 cell was used as a cell model, in which the O-GlcNAcylated proteins have been considered as potential tumor markers,[4,16] to achieve the in situ simultaneous detection of intracellular O-GlcNAcylated proteins and total GlcNAc groups.

EXPERIMENTAL SECTION

Materials and Reagents. FITC-labeled succinylated wheat germ agglutinin (FSWGA) was purchased from Vector Laboratories (USA). Alloxan, sodium butyrate (NaBu), *O*-(2-acetamido-2-deoxy-D-glucopyranosylidenamino) *N*-phenylcarbamate (PUGNAc), cysteine, glucose, *N*-acetylglucosamine (GlcNAc), and poly-*N*-acetylglucosamine (PGlcNAc) were purchased from Sigma-Aldrich Inc. (USA). Tetraacetylated *N*-azidoacetylglucosamine (TAcGlcNAz), Alexa Fluor 647 DIBO alkyne, Cell Light Lysosomes-RFP, BacMam 2.0, Opti-MEM reduced serum medium, lipofectamine RNAiMAX (Lipo), P-phycoerythrin (PE) conjugated E-cadherin antibody, and PE conjugated epithelial cell adhesion molecule (EpCAM) antibody were obtained from Life Technologies (USA). Recombinant human p53 protein was purchased from ABCAM (UK). Chloroauric acid ($HAuCl_4 \cdot 4H_2O$) was obtained from Shanghai Chemical Reagent Company (Shanghai, China). Trisodium citrate was obtained from Sinopharm Chemical Reagent Co., Ltd. (China). Thiol polyethylene glycol 5000 folic acid (HS-PEG-FA) was obtained from Ponsure Biotechnology Ltd. (Shanghai, China). Sodium methoxide and 4′,6-diamidino-2-phenylindole (DAPI) were obtained from Titan Technology Co., Ltd. (Shanghai, China). MCF-7 and HaCaT cells were from KeyGen Biotech. Co. Ltd. (Nanjing, China). Phosphate buffer saline (PBS, pH 7.4) contained 136.7 mM NaCl, 2.7 mM KCl, 8.72 mM Na_2HPO_4, and 1.41 mM KH_2PO_4. For lectin-carbohydrate interaction, 0.1 mM $CaCl_2$ and 0.1 mM $MnCl_2$ were added in PBS. Cell lysis buffer contained 10 mM Tris-HCl (pH 7.4), 1 mM $MgCl_2$, 1 mM EDTA, 0.1 mM PMSF, 0.5% CHAPS and 10% Glycerol. All other reagents were of analytical grade. All aqueous solutions were prepared using ultrapure water (≥18 MΩ, Milli-Q, Millipore).

OGT shRNA 1, 5′-GCCCTAAGTTTGAGTCCAAATCTCGAGATTTGGACTCAAACTTAGGGC-3′, OGT shRNA 2, 5′-GCTGAGCAGTATTCCGAGAAACTCGAGTTTCTCGGAATACTGCTCAGC-3′, and scrambled shRNA, 5′-CCTAAGGTTAAGTCGCCCTCGCTCTAGCGAGGGCGACTTAACCTT-3′ were synthesized by Shanghai GenePharma Co. Ltd. (Shanghai, China) and all carried by plasmid vector pGPU6.

Apparatus. The UV absorption spectra were recorded on an UV-3600 UV−vis−NIR spectrophotometer (Shimadzu Company, Japan). The fluorescence spectra were recorded on an F-7000 fluorescence spectrophotometer (Hitachi, Japan). Transmission electron microscopic (TEM) imaging was performed on a JEM-2800 high throughput electron microscope (JEOL, Japan). Dynamic light scattering (DLS) and Zeta potential measurements were performed on a NanoZS90Plus particle/protein size and Zeta potential analyzer (Brookhaven, USA). Flow cytometric analysis was performed on a Coulter FC-500 flow cytometer (Beck-man Coulter, USA). The fluorescence cell imaging was performed on a TCS SP5 laser scanning confocal microscope (Leica, Germany). The cell numbers were determined using a Countess II FL Automated Cell Counter (Life Technologies, USA). The absorbance in MTT assay was recorded on a Varioskan Flash multimode reader (ThermoFisher Scientific, USA).

Cell Culture. MCF-7 and HaCaT cells were cultured at 37 °C in RPMI 1640 medium (GIBCO) and DMEM medium (GIBCO) supplemented with 10% fetal calf serum (FCS, Sigma), penicillin (100 μg/mL) and streptomycin (100 μg/mL) in a humidified atmosphere containing 5% CO_2, respectively.

Preparation of Functional Dual-Color Indicator. PGAu were synthesized by quickly adding 1.25 mL trisodium citrate (1%) to 50 mL boiling $HAuCl_4$ solution (0.01%) containing 100 μL PGlcNAc (10 mg/mL) under continuous stirring.[17] The reaction mixture was stirred at 100 °C for 15 min until the color turned red or purple. The mixture was cooled down to room temperature and then stored at 4 °C. Prior to use, PGAu were washed by centrifugation at 12000 rpm and resuspended in PBS. The concentration of PGAu was determined from the UV−vis absorption spectrum.[18]

TAcGlcNAz was dissolved in methanol containing a catalytic amount of sodium methoxide for deacetylation. The reaction was closely followed by TLC and could be completed after 1 h at room temperature. The reaction mixture was subsequently neutralized by dropwise adding a dilute methanol solution of acetic acid (pH 4.0) until pH 7.0. The obtained N-azidoacetylglucosamine (GlcNAz) was then diluted in PBS and mixed with Alexa Fluor 647 DIBO alkyne at 1:1 mol ratio. After 15 min copper-free click reaction between azido and DIBO at room temperature, the Alexa Fluo 647 labeled GlcNAc (FGlcNAc) was obtained.

Ten microliters FSWGA (100 μM), 10 μL HS-PEG-FA (100 μM), and 10 μL tween (1%) were added into 1 mL PGAu (10 nM). After shaking overnight on a vertical rotary mixing device, the mixture was centrifuged at 12000 rpm for 5 min, and the

DOI: 10.1021/acs.analchem.7b03587
Anal. Chem. 2018, 90, 3073−3078

nanoparticles were redispersed in 1 mL of PBS. Ten μL of FGlcNAc (100 μM) and 10 μL of tween (1%) were then added into the resulting solution and subjected to shaking on a vertical rotary mixing device for 4 h. The obtained functional dual-color indicator probe was redispersed in 1 mL of PBS.

In Vitro Verification of the Competitive Release from the Indicator. MCF-7 cells with a concentration of 7.5×10^5 cells/mL were dispersed in cell lysis buffer. After vortexing on ice for 2 h, the mixture was centrifuged at 12000 rpm for 15 min to obtain the supernatant as the cell lysis of MCF-7 cells. The sample of O-GlcNAcylated protein could be obtained by filtering the cell lysis with a 10 kd ultrafilter to remove the intracellular small molecules such as GlcNAc. 50 μL cysteine (10 mg/mL), 50 μL glucose (10 mg/mL), 50 μL GlcNAc (10 mg/mL), 50 μL p53 protein (100 μg/mL), 50 μL ultrafiltered cell lysis (7.5×10^5 cells/mL) and 50 μL cell lysis (7.5×10^5 cells/mL) were added into 100 μL of 10 nM probe, respectively. After incubation at 37 °C for 4 h, the mixtures were subject to fluorescent detection, respectively.

MTT Assay of Cell Viability. The viability of MCF-7 cells during the probe treatment was tested by MTT assay. Briefly, after MCF-7 cells (100 μL, 1.0×10^5 cells/mL) were seeded in the wells of 96-well plate for 12 h, they were washed with PBS twice and subjected to incubation with 10 nM probe for different times. Meanwhile, the MCF-7 cells without treatment were incubated in culture medium as control. After these cells were incubated with MTT (50 μL, 1 mg/mL) for 4 h at 37 °C, 100 μL of dimethyl sulfoxide was added to each well with vibration for 15 min at room temperature to dissolve the crystals formed by the cells. Finally, the absorbance of each well was measured using a Varioskan Flash multimode reader. The relative cell viability (%) was calculated by $(A_{test}/A_{control}) \times 100$.

Colocalization Imaging. For nuclear colocalization imaging, the confocal dishes seeded with MCF-7 cells were first incubated with 200 μL of 8 nM probe in PBS at 37 °C. After 4-h incubation, the cells were washed with PBS twice to remove extra probe and then incubated with 200 μL DAPI (10 μg/mL) in PBS for 10 min. The cells were washed with PBS twice to perform confocal fluorescence imaging. For lysosome colocalization imaging, the confocal dishes seeded with MCF-7 cells were first incubated with 200 μL Cell Light Lysosomes-RFP BacMam 2.0 (1×10^6 particles/mL) at 37 °C. After one-night incubation, the cells were washed with PBS twice and then incubated with 200 μL of 8 nM probe in PBS at 37 °C for 4 h. The cells were washed with PBS twice to perform confocal fluorescence imaging.

Regulation of Intracellular O-GlcNAcylation. The confocal dishes seeded with MCF-7 cells were first incubated with 10 mM alloxan, GlcNAc or PUGNAc in Opti-MEM reduced serum medium in cell culture box. After 24-h incubation, the cells were washed with Opti-MEM reduced serum medium twice and incubated with 200 μL of 8 nM probe in PBS at 37 °C for 4 h. The cells were washed with PBS twice for confocal fluorescence imaging.

RNA Interference. The MCF-7 cells seeded in confocal dishes were transfected with 50 ng/μL shRNA using Lipo in Opti-MEM reduced serum medium for 24 h at 37 °C according to the manufacturer's protocol. After the cells were washed twice with Opti-MEM reduced serum medium, they were incubated with 200 μL of 8 nM probe in PBS at 37 °C for 4 h. The cells were washed with PBS twice for confocal fluorescence imaging.

Flow Cytometric Analysis of Intracellular GlcNAc and Cell Surface Proteins. After MCF-7 cells (1×10^6 cells/mL) were incubated with different concentrations of probe or different kinds of antibody in PBS at 37 °C for different times, the cells were washed with PBS twice to perform flow cytometric analysis. The MCF-7 cells treated with different reagents were subjected to flow cytometric analysis with same procedure.

RESULTS AND DISCUSSION

Construction of Dual-Color Indicator. The assembly of FSWGA on PGAu was first demonstrated with UV and fluorescence spectra. After the PGAu was incubated with FSWGA, the resulting PGAu-FSWGA showed an extra characteristic peak of FSWGA protein at 280 nm (Figure S1A), while both the supernatants in the absence or presence of HS-PEG-FA showed similar decrease of FITC fluorescent intensity around 516 nm compared with the initial FSWGA solution due to specific sugar-lectin interaction between PGAu and FSWGA (Figures S1B and S2A), indicating the similar amount of FSWGA conjugated to PGAu. To verify the specific interaction between FSWGA and PGAu, bare gold nanoparticles and polysialic acid coated gold nanoparticles (PSAu) were incubated with FSWGA, which did not obviously decrease the FITC fluorescent intensity of the supernatants due to the lack of recognition specificity (Figure S1B). The shape uniformity of the AuNPs, PGAu and PGAu-FSWGA was confirmed by TEM images (Figure S1C–E). DLS analysis indicated the increased hydrated-sizes of the nanoparticles following the sequence: AuNPs < PGAu < PGAu-FSWGA (Figure S1F–H), which further demonstrated the successful assembly of FSWGA on PGAu, and good stability of PGAu-FSWGA.

FGlcNAc was synthesized by copper-free click reaction between Alexa Fluor 647 DIBO alkyne and GlcNAz,[19−21] which was obtained by deacetylation of TAcGlcNAz.[22] After FGlcNAc was mixed with HS-PEG-FA and FSWGA conjugated PGAu (PGAu-FA/FSWGA) to incubate for 4 h, obvious fluorescent intensity decrease of Alexa Fluo 647 around 666 nm could be observed from the supernatant due to the conjugation of FGlcNAc to PGAu-FA/FSWGA (Figure S2B). From the fluorescent intensities of the two supernatants and the standard curves for FSWGA and FGlcNAc (Figure S3), the number of FSWGA and FGlcNAc assembled on each indicator probe could be calculated to be about 126 and 117 respectively. The change of zeta potential during step-by-step assembly of the probes further confirmed the successful conjugation (Figure S4).

In Vitro Verification of Dynamic Competition. To investigate the competitive release ability of the designed indicator, it was incubated with GlcNAc, human p53 protein (a model O-GlcNAcylated protein)[8] and cell lysis in vitro, respectively. The cell lysis contained both O-GlcNAcylated proteins and the dissociated GlcNAc residue. After cell lysis was ultrafiltered with a 10 kd ultrafilter to remove the intracellular small molecules such as GlcNAc, the sample of O-GlcNAcylated proteins could be obtained. The probe did not exhibit any self-fluorescence due to the inherent quenching effect of AuNPs (Figure S2). It kept nonfluorescent when incubated with cysteine (the main biogenic thiol inside cell) or glucose, indicating its stability to biogenic thiol and specificity to GlcNAc (Figure 2A and 2B). But the mixture of the probe with cell lysis showed obvious green and red fluorescence of

DOI: 10.1021/acs.analchem.7b03587
Anal. Chem. 2018, 90, 3073−3078

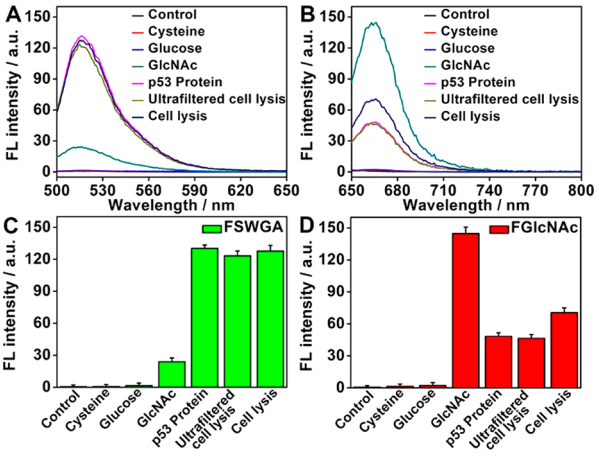

Figure 2. (A, B) Fluorescence spectra of probe (control), and probes treated with cysteine, glucose, GlcNAc, p53 protein, ultrafiltered cell lysis and cell lysis in the emission range of (A) FITC and (B) Alexa Fluor 647 respectively. (C, D) Peak intensities at (C) 516 and (D) 666 nm from (A) and (B) respectively.

both FITC and Alexa Fluo 647 after incubation at 37 °C for 4 h, which indicated the release of FSWGA and FGlcNAc due to the competitive conjugation of intracellular O-GlcNAcylated proteins and dissociated GlcNAc residue to FSWGA in the probe. Furthermore, the green fluorescence from the released FSWGA was similar to that incubated with p53 protein and ultrafiltered cell lysis, and the latter two mixtures showed weaker red fluorescence from released FGlcNAc (Figure 2C and 2D). Interestingly, the incubation of the probe with GlcNAc exhibited only the strong red fluorescence from the released FGlcNAc, while the green fluorescence of FSWGA was very weak. Thus, it was reasonable to conclude that the competitive conjugation of O-GlcNAcylated proteins to FSWGA resulted in the release of the conjugate of FSWGA with FGlcNAc from the probe, and the competitive binding of GlcNAc and dissociated GlcNAc residue to FSWGA released only FGlcNAc.

The competitive binding resulted from the one or few GlcNAc-binding sites on the dimeric-subunit structure of FSWGA.[15] At a thermodynamic equilibrium state, the dissociated GlcNAc residue bound only the outside subunit of FSWGA, while O-GlcNAcylated proteins preferred to the inside subunit of FSWGA due to the ligand confinement of the subunits on PGAu surface[23−25] and the different mobility of O-GlcNAcylated proteins and dissociated GlcNAc residue. The dissociated GlcNAc residue with high mobility had priority to replace FGlcNAc at the lowly confined outside subunit, while O-GlcNAcylated proteins with low mobility would replace PGlcNAc at the highly confined inside subunit, which released the conjugate of FSWGA with FGlcNAc. Thus, the green fluorescence of FSWGA could be used to monitor the level of O-GlcNAcylated proteins, while the red fluorescence of FGlcNAc was related to both the released FGlcNAc and the released conjugate of FSWGA with FGlcNAc, and thus the sum of dissociated GlcNAc residue and O-GlcNAcylated proteins. This mean the dissociated GlcNAc residue could also been monitored from the relative changes of fluorescence intensity of both FITC and Alexa Fluor 647.

Intracellular Delivery of Indicator. To obtain high-quality image for sensitive visual monitoring, the probe concentration and incubation time were optimized to be 8 nM (Figure S5) and 4 h (Figure S6) by confocal fluorescence imaging and flow cytometric analysis. The probe incubation did not influence cell viability (Figure S7). The feasibility of FA receptor-mediated cell endocytosis of the probe[26,27] was demonstrated by comparing confocal fluorescence images of FA-acceptor abundant MCF-7 and FA-acceptor lacking HaCaT cells after incubation with the probes in the presence and absence of FA (Figure S8 and S9). TEM image of probe treated MCF-7 cell further confirmed the successful delivery of probe into cell (Figure S10).

The location of probe in cells was investigated by the colocalization imaging of nuclear and lysosomes. The nuclear and lysosomes in MCF-7 cells were dyed with DAPI and lysosomes-RFP, which were excited at 405 and 543 nm and did not influence the excitation of FITC (488 nm) and Alexa Fluo 647 (633 nm), respectively (Figure S11). The dyed cells were then incubated with 8 nM probe for 4 h and subjected to confocal fluorescence imaging, respectively. The fluorescence from the probe observed with G and R channels could overlap in both colocalization images (Figure 3), however they did not

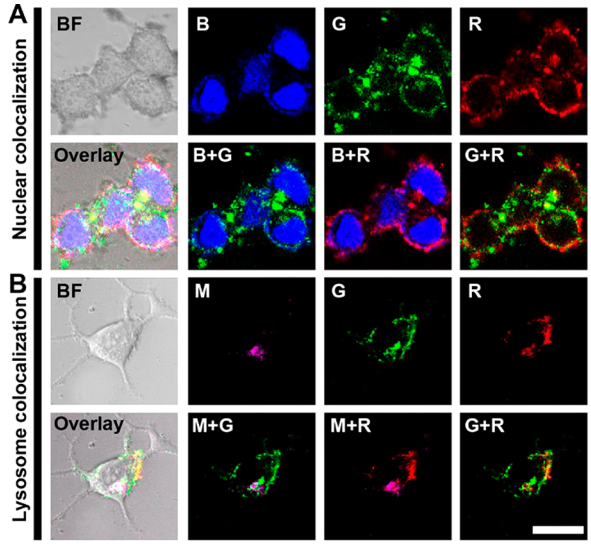

Figure 3. (A) Confocal nuclear and (B) confocal lysosome colocalization imaging. BF: Bright field. B: Bule channel of DAPI. M: Mauve channel of RFP. G: Green channel of FITC. R: Red channel of Alexa Fluor 647. Scale bar: 20 μm.

overlap with the fluorescence from DAPI dyed nuclear observed with B channel (Figure 3A), indicating that no probe entered into the nuclear. Meanwhile, a large area of G- and R-channel fluorescence from the probe was beyond the fluorescence area from lysosomes-RFP dyed lysosomes observed with M channel, and only part overlapping was observed (Figure 3B), which indicated that most probe were dispersed in cytoplasm, and only a negligible amount of probe was caged in the lysosome. The latter did not affect the qualitative monitoring results. Thus, the designed functional dual-color indicator located in cytoplasm and could be used to in situ monitor the targets in cytoplasm.

Monitoring of Intracellular O-GlcNAcylation Regulation. The level of O-GlcNAcylation in living cells can be regulated with different OGT shRNAs,[28] such as OGT shRNA 1 and OGT shRNA 2, and alloxan as OGT inhibitor,[29] and PUGNAc as OGA inhibitor,[30−32] and exogenous GlcNAc. The OGT shRNAs can lead to more than 50% knockdown of

DOI: 10.1021/acs.analchem.7b03587
Anal. Chem. 2018, 90, 3073−3078

OGT.[28] After MCF-7 cells were treated with OGT shRNA 1, OGT shRNA 2, or alloxan and then incubated with 8 nM probe for 4 h, obvious decrease of green fluorescence was observed in the confocal fluorescence images, while the change of red fluorescence was negligible compared with scrambled shRNA treated and untreated cells (Figure 4), indicating that the total

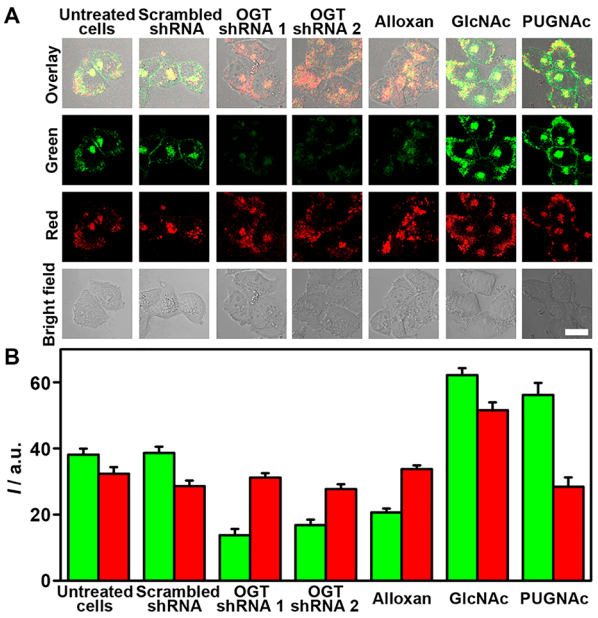

Figure 4. (A) Confocal fluorescence images of untreated, scrambled shRNA, OGT shRNA 1, OGT shRNA 2, alloxan, GlcNAc, and PUGNAc treated MCF-7 cells after incubation with 8 nM probe for 4 h. Scale bar: 20 μm. (B) Mean intensity of green and red channel obtained from (A).

amount of intracellular GlcNAc groups was stable, and the equilibrium of OGT/OGA mediated O-GlcNAcylation tilted to less O-GlcNAcylated proteins. Contrarily, the treatment of PUGNAc led to increasing green fluorescence due to the inhibited dissociation of O-GlcNAcylated proteins, which kept higher level of O-GlcNAcylated proteins at the same total amount of intracellular GlcNAc groups. However, the treatment of exogenous GlcNAc increased both red and green fluorescence due to the increasing amount of GlcNAc in cytoplasm, which produced more O-GlcNAcylated proteins due to the O-GlcNAcylation equilibrium. These results were verified by flow cytometric analysis (Figure S12), which indicated the feasibility of the indicator for simultaneous monitoring of the level of O-GlcNAcylated proteins and total amount of GlcNAc groups in cell.

Practicality of Dual-Color Imaging Strategy. Poor-differentiated cells are more invasive than well-differentiated cells,[33] thus the biological relativity investigation of differentiation-related proteins on cancer cell surface with intracellular O-GlcNAcylation is important for revealing glycosylation-related biological processes and potential tumor progression. Here, two typical cell epithelial proteins, E-cadherin and EpCAM on MCF-7 cells, which can respectively suppress invasion[34] or enhance proliferation of cancer cells,[35] were used as the model of differentiation-related proteins. They could be visually monitored with corresponding PE conjugated antibodies by exciting the PE at 514 nm, which did not interfere with the excitation of FITC (488 nm) and Alexa Fluo 647 (633 nm), respectively (Figure S11). Thus, the biological relativity of intracellular O-GlcNAcylation with cell surface E-cadherin and EpCAM could be investigated by the designed dual-color imaging strategy and the PE fluorescence (Figure 5A). After

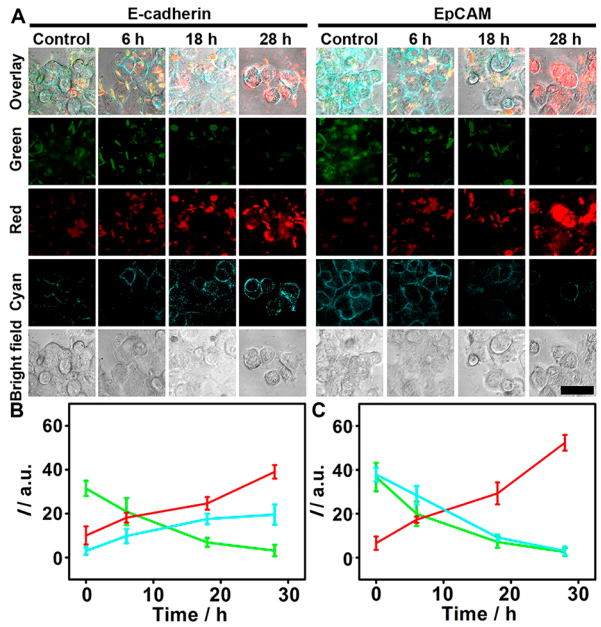

Figure 5. (A) Confocal fluorescence images of MCF-7 cells treated with 5 mM NaBu for 0, 6, 18, and 28 h after incubation with 8 nM probe for 4 h and then 20% PE conjugated E-cadherin or EpCAM antibody in PBS for 30 min. Scale bar: 40 μm. (B, C) Mean intensity of green, red, and cyan channels obtained from panel A.

MCF-7 cells were subjected to 0, 6, 18 and 28-h treatment with 5 mM NaBu, an antitumor drug to induce better differentiation of tumor cells,[36,37] the treated cells were incubated with 8 nM probe for 4 h and then 20% PE conjugated E-cadherin or EpCAM antibody for 30 min. With the increasing treatment time, the bright field images showed obviously better differentiation of MCF-7 cells (Figure S13), both the green FITC fluorescence positively related to intracellular O-GlcNAcylated proteins and the PE fluorescence from the labeled EpCAM (Figure 5C) decreased, while the red Alex 647 fluorescence positively related to intracellular total GlcNAc and the PE fluorescence from the labeled E-cadherin (Figure 5B) increased. These results were verified by flow cytometric analysis (Figure S14), indicating that the level of O-GlcNAcylated proteins decreased while the total GlcNAc groups increased. This was consistent with the fact that better differentiated cells have significantly lower OGT expression and higher OGA expression.[38] Besides, the increasing total GlcNAc groups along with better differentiation of MCF-7 cells implied the relativity of the intracellular GlcNAc synthesis with cell surface E-cadherin and EpCAM expression.

CONCLUSION

This work designs a functional dual-color indicator and proposes a simple technique for simultaneously in situ monitoring the level of intracellular O-GlcNAcylated proteins and the total amount of GlcNAc groups in living cells through one-step incubation. This indicator can be constructed by simply assembling HS-PEG-FA and FSWGA and then FGlcNAc on PGAu. This technique can be conveniently performed by incubating the cells with the indicator and then

DOI: 10.1021/acs.analchem.7b03587
Anal. Chem. 2018, 90, 3073−3078

observing the change of lighted-up fluorescence. Due to the different ligand confinement of FSWGA subunits on the indicator and different mobility of the targets, the competitive binding of different targets with different subunits of FSWGA releases different dye-labeled species and thus lights up the fluorescence from FSWGA and/or FGlcNAc. This proposed protocol has been successfully used for investigating the OGT/OGA mediated O-GlcNAcylation equilibrium and the biological relativity between intracellular O-GlcNAcylation and cell surface differentiation-related proteins during drug treatment. It can be easily extended to other intracellular glycosylation cycles by changing the labeled lectin and the corresponding carbohydrate, demonstrating its practicality for research of glycosylation equilibrium and related biological processes.

■ ASSOCIATED CONTENT

Supporting Information

The Supporting Information is available free of charge on the ACS Publications website at DOI: 10.1021/acs.analchem.7b03587.

UV and fluorescence spectra of probes, flow cytometric data and fluorescence images of cells, and optimization of conditions (PDF)

■ AUTHOR INFORMATION

Corresponding Author

*Phone/Fax: +86-25-89683593. E-mail: hxju@nju.edu.cn.

ORCID

Yunlong Chen: 0000-0002-3775-3028

Lin Ding: 0000-0001-5381-3484

Huangxian Ju: 0000-0002-6741-5302

Notes

The authors declare no competing financial interest.

■ ACKNOWLEDGMENTS

This work was financially supported by National Natural Science Foundation of China (21605080, 21635005, 21611130176, 21361162002, 91413118), and Natural Science Foundation of Jiangsu Province (BK20160646).

■ REFERENCES

(1) *Essentials of Glycobiology*, 2nd ed.; Varki, A., Cummings, R. D., Esko, J. D., Freeze, H. H., Stanley, P., Bertozzi, C. R., Hart, G. W., Etzler, M. E., Eds.; Cold Spring Harbor Laboratory Press: Cold Spring Harbor, NY, 2009.

(2) Wells, L.; Vosseller, K.; Hart, G. W. *Science* **2001**, *291*, 2376−2378.

(3) Hart, G. W.; Housley, M. P.; Slawson, C. *Nature* **2007**, *446*, 1017−1022.

(4) Chaiyawat, P.; Netsirisawan, P.; Svasti, J.; Champattanachai, V. *Front. Endocrinol.* **2014**, *5*, 193.

(5) Kreppel, L. K.; Blomberg, M. A.; Hart, G. W. *J. Biol. Chem.* **1997**, *272*, 9308−9315.

(6) Gao, Y.; Wells, L.; Comer, F. I.; Parker, G. J.; Hart, G. W. *J. Biol. Chem.* **2001**, *276*, 9838−9845.

(7) Comer, F. I.; Hart, G. W. *J. Biol. Chem.* **2000**, *275*, 29179−29182.

(8) Doll, F.; Buntz, A.; Späte, A.-K.; Schart, V. F.; Timper, A.; Schrimpf, W.; Hauck, C. R.; Zumbusch, A.; Wittmann, V. *Angew. Chem., Int. Ed.* **2016**, *55*, 2262−2266.

(9) Ma, J.; Hart, G. W. *Clin. Proteomics* **2014**, *11*, 8.

(10) Monsigny, M.; Sene, C.; Obrenovitch, A.; Roche, A.-C.; Delmotte, F.; Boschetti, E. *Eur. J. Biochem.* **1979**, *98*, 39−45.

(11) Wright, C. S. *J. Mol. Biol.* **1989**, *209*, 475−487.

(12) Harata, K.; Nagahora, H.; Jigami, Y. *Acta Crystallogr., Sect. D: Biol. Crystallogr.* **1995**, *51*, 1013−1019.

(13) Schwefel, D.; Maierhofer, C.; Beck, J. G.; Seeberger, S.; Diederichs, K.; Möller, H. M.; Welte, W.; Wittmann, V. *J. Am. Chem. Soc.* **2010**, *132*, 8704−8719.

(14) Wright, C. S.; Kellogg, G. E. *Protein Sci.* **1996**, *5*, 1466−1476.

(15) Rice, R. H.; Etzler, M. E. *Biochemistry* **1975**, *14*, 4093−4099.

(16) Gu, Y. C.; Mi, W. Y.; Ge, Y. Q.; Liu, H. Y.; Fan, Q.; Han, C. F.; Yang, J.; Han, F.; Lu, X. Z.; Yu, W. G. *Cancer Res.* **2010**, *70*, 6344−6351.

(17) Frens, G. *Nature, Phys. Sci.* **1973**, *241*, 20−22.

(18) Haiss, W.; Thanh, N. T. K.; Aveyard, J.; Fernig, D. G. *Anal. Chem.* **2007**, *79*, 4215−4221.

(19) Ning, X. H.; Guo, J.; Wolfert, M. A.; Boons, G. J. V. *Angew. Chem., Int. Ed.* **2008**, *47*, 2253−2255.

(20) Jewett, J. C.; Sletten, E. M.; Bertozzi, C. R. *J. Am. Chem. Soc.* **2010**, *132*, 3688−3690.

(21) Baskin, J. M.; Prescher, J. A.; Laughlin, S. T.; Agard, N. J.; Chang, P. V.; Miller, I. A.; Lo, A.; Codelli, J. A.; Bertozzi, C. R. *Proc. Natl. Acad. Sci. U. S. A.* **2007**, *104*, 16793−16797.

(22) Gloster, T. M.; Zandberg, W. F.; Heinonen, J. E.; Shen, D. L.; Deng, L.; Vocadlo, D. J. *Nat. Chem. Biol.* **2011**, *7*, 174−181.

(23) Young, T.; Abel, R.; Kim, B.; Berne, B. J.; Friesner, R. A. *Proc. Natl. Acad. Sci. U. S. A.* **2007**, *104*, 808−813.

(24) Tagliazucchi, M.; Szleifer, I. *J. Am. Chem. Soc.* **2015**, *137*, 12539−12551.

(25) Low-Nam, S. T.; Lidke, K. A.; Cutler, P. J.; Roovers, R. C.; van Bergen en Henegouwen, P. M. P.; Wilson, B. S.; Lidke, D. S. *Nat. Struct. Mol. Biol.* **2011**, *18*, 1244−1249.

(26) Xie, R.; Hong, S.; Feng, L.; Rong, J.; Chen, X. *J. Am. Chem. Soc.* **2012**, *134*, 9914−9917.

(27) Santra, S.; Kaittanis, C.; Santiesteban, O. J.; Perez, J. M. *J. Am. Chem. Soc.* **2011**, *133*, 16680−16688.

(28) Caldwell, S. A.; Jackson, S. R.; Shahriari, K. S.; Lynch, T. P.; Sethi, G.; Walker, S.; Vosseller, K.; Reginato, M. J. *Oncogene* **2010**, *29*, 2831−2842.

(29) Lenzen, S.; Panten, U. *Diabetologia* **1988**, *31*, 337.

(30) Haltiwanger, R. S.; Grove, K.; Philipsberg, G. A. *J. Biol. Chem.* **1998**, *273*, 3611−3617.

(31) Dong, D. L.; Hart, G. W. *J. Biol. Chem.* **1994**, *269*, 19321−19330.

(32) Horsch, M.; Hoesch, L.; Vasella, A.; Rast, D. M. *Eur. J. Biochem.* **1991**, *197*, 815−818.

(33) Frixen, U. H.; Behrens, J.; Sachs, M.; Eberle, G.; Voss, B.; Warda, A.; Löchner, D.; Birchmeier, W. *J. Cell Biol.* **1991**, *113*, 173−185.

(34) Vleminckx, K.; Vakaet, L., Jr; Mareel, M.; Fiers, W.; Van Roy, F. *Cell* **1991**, *66*, 107−119.

(35) Münz, M.; Kieu, C.; Mack, B.; Schmitt, B.; Zeidler, R.; Gires, O. *Oncogene* **2004**, *23*, 5748−5758.

(36) Hao, P. P.; Lee, M. J.; Yu, G. R.; Kim, I. H.; Cho, Y. G.; Kim, D. G. *Mol. Cells* **2013**, *36*, 424−431.

(37) Foglietta, F.; Serpe, L.; Canaparo, R.; Vivenza, N.; Riccio, G.; Imbalzano, E.; Gasco, P.; Zara, G. P. *J. Pharm. Pharm. Sci.* **2014**, *17*, 231−247.

(38) Krześlak, A.; Forma, E.; Bernaciak, M.; Romanowicz, H.; Bryś, M. *Clin. Exp. Med.* **2012**, *12*, 61−65.

DOI: 10.1021/acs.analchem.7b03587
Anal. Chem. 2018, 90, 3073−3078